Supporting information for:
Strengthening poly(lactic acid) composites with poly(methyl methacrylate) functionalized flax nanofibrils

Authors:

Abigail Mulligan,[a] Ahmad A. L. Ahmad,[a,b,†] Peter V. Kelly,[a,‡] Siamak Shams Es-haghi,[b,c] Peng Cheng,[a] Amber M Hubbard,[d] Kathryn Slavny,[d,e] Meghan E Lamm,[d] Sanjita Wasti,[d] William M. Gramlich[a,b,f,*]

[a] Department of Chemistry, University of Maine, Orono, Maine 04469, USA

[b] Advanced Structures and Composites Center, University of Maine, Orono, Maine 04469, USA

[c] Department of Chemical and Biomedical Engineering, University of Maine, Orono, Maine 04469-5737, USA

[d] Manufacturing Science Division, Oak Ridge National Laboratory, Oak Ridge, Tennessee, 37830, USA

[e] ORISE Participant in the U.S. Department of Energy Education Collaboration at ORNL Program, Oak Ridge, Tennessee, 37830, USA

[f] Forest Bioproducts Research Institute, University of Maine, Orono, Maine 04469, USA

*Corresponding author: william.gramlich@maine.edu

† Current address: Department of Allied Medical Sciences, Technical College, Jadara University, Irbid, 21110, Jordan

‡ Current address: Department of Materials Science and Engineering, Cornell University, Ithaca, New York, 14850, USA

Additional Methods Detail

Dynamic Mechanical Analysis (DMA):

A TA Instruments DMA 850 was used for all testing, where samples were rectangular in shape with dimensions of 60 mm x 10 mm x 3 mm (l x w x h). Initially, amplitude and frequency sweeps were performed for each material at 30 °C to ensure that testing was performed within the linear viscoelastic regime. Secondarily, temperature sweeps were performed for each material from 30 °C to 120 °C at a temperature ramp rate of 3 °C min^{-1}, a frequency of 1 Hz, and an amplitude of 15 μm. A minimum of 2 temperature sweeps were performed for each composite formulation.

Thermogravimetric Analysis (TGA):

A TA Instruments TGA 5500 was used for all testing. Temperature ramps were performed for all composite formulations where the temperature was ramped from 30 °C to 600 °C at a temperature ramp rate of 10 °C min^{-1} in an air environment. The temperature at which a 2 wt.% mass loss was recorded as $T_{2\%}$ and the onset of thermal degradation was recorded as T_{onset}. A minimum of 3 experiments were performed for each composite formulation to ensure statistical significance.

Differential Scanning Calorimetry (DSC):

A TA Instruments DSC 2500 was used for all testing where a minimum of 3 samples were tested for each composite formulation to ensure statistical significance. A heat-cool-heat experiment was performed with a lower temperature of 0 °C and an upper temperature of 200 °C at a temperature ramp rate of 10 °C min^{-1}. The glass transition temperature (T_g) and the cold crystallization temperatures (T_{cc}) were recorded from the second heating curve in all cases. In addition, the crystallinity (X) was calculated from the second heating curve for all composite formulations, as seen in previous publications from this team.

Pycnometry:

The density for all samples was collected using a Micromeritics AccuPyc 1340 II pycnometer according to ASTM D-3576, where all tests were performed under a hydrogen environment. Sample masses were kept constant between 0.2 – 0.3 g and a minimum of 3 samples were run for each composite formulation to ensure statistical significance. The sample volume (cm^3) and density (g cm^{-3}) were recorded over 5 cycles for each individual run.

Scanning Electron Microscopy (SEM):

To understand the dispersion of fibers and interface between fiber and matrix, the cross section of the composites was potted, polished and observed under the Zeiss Merlin field emission scanning electron microscope at an accelerating voltage of 1 kV. The detailed procedure of potting and polishing can be found elsewhere. All the samples were sputter coated with iridium.

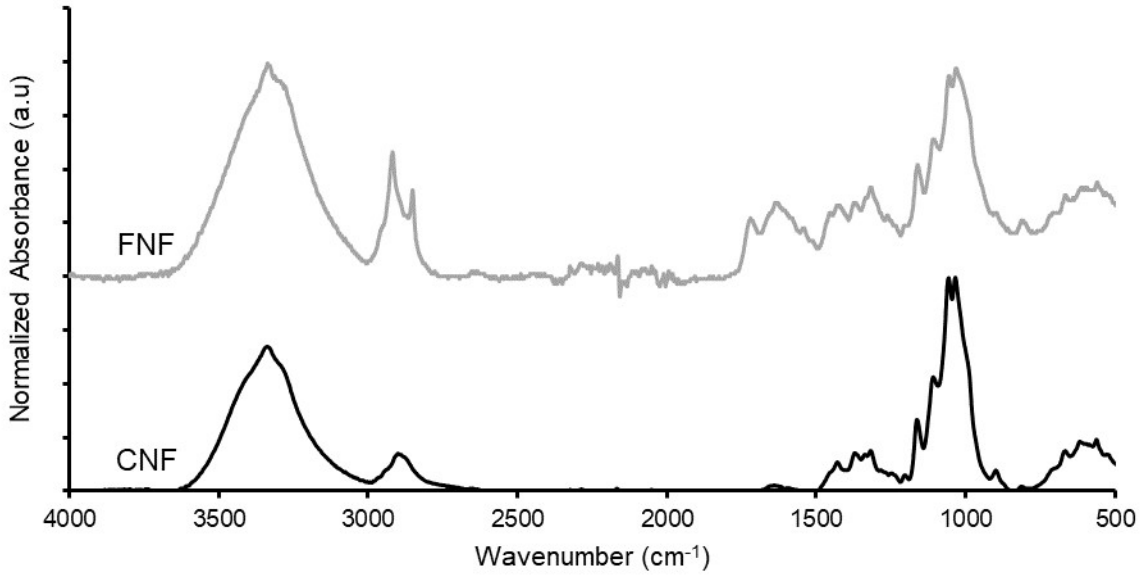

Figure S1. ATR-FTIR spectra of dried flax nanofibrils (FNFs) and cellulose nanofibrils (CNFs). Spectra are normalized to 1055 cm^{-1} band and shifted vertically to improve visibility. Bands in the FNF spectrum at 2915 and 2850 cm^{-1} correspond to the CH_2 stretches of fatty acids and at 1615 and 1425 cm^{-1} correspond to lignin.

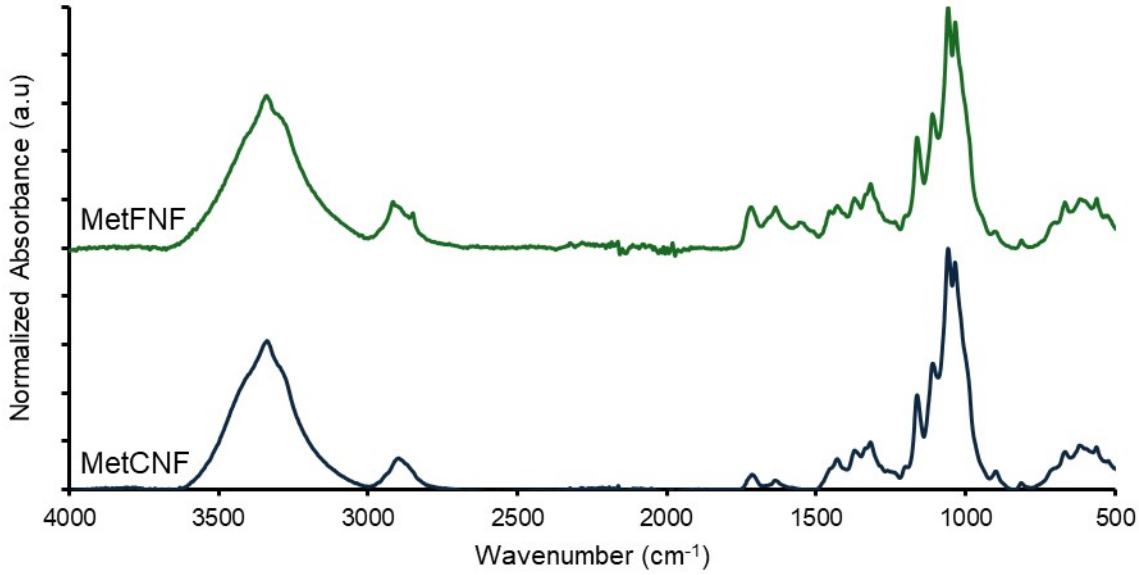

Figure S2. ATR-FTIR spectra of dried methacrylated FNFs (MetFNFs) and methacrylated CNFs (MetCNFs). Spectra are normalized to 1055 cm^{-1} band and shifted vertically to improve visibility.

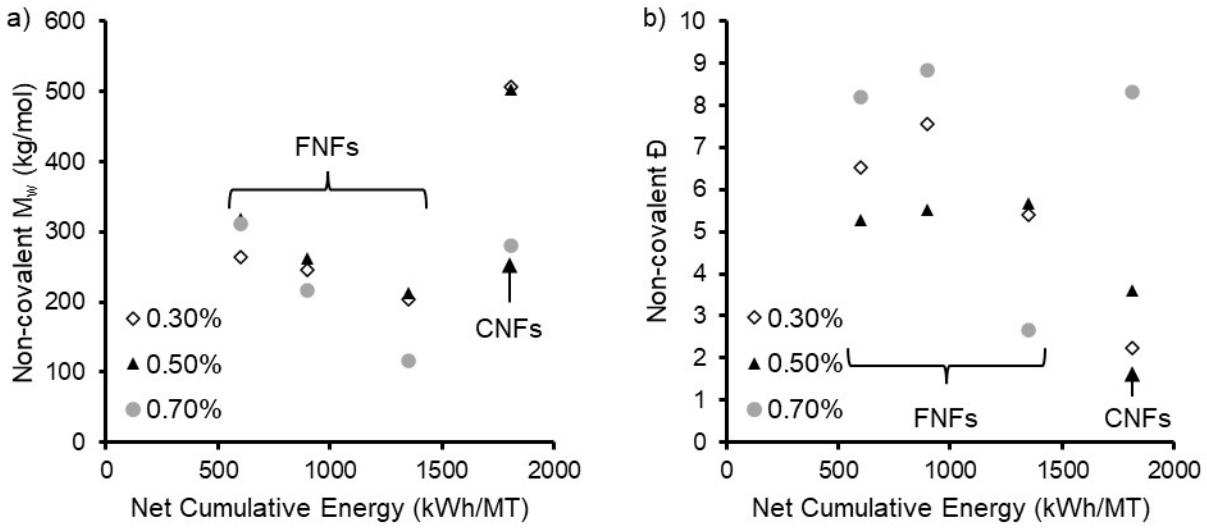

Figure S3. a) Weight average molecular weight (M_w) and b) dispersity (Đ) of non-covalently bound PMMA on PMMA-modified materials as a function of net cumulative energy used to refine into nanomaterials and for different wt% of FNFs or CNFs in suspension during the polymerization.

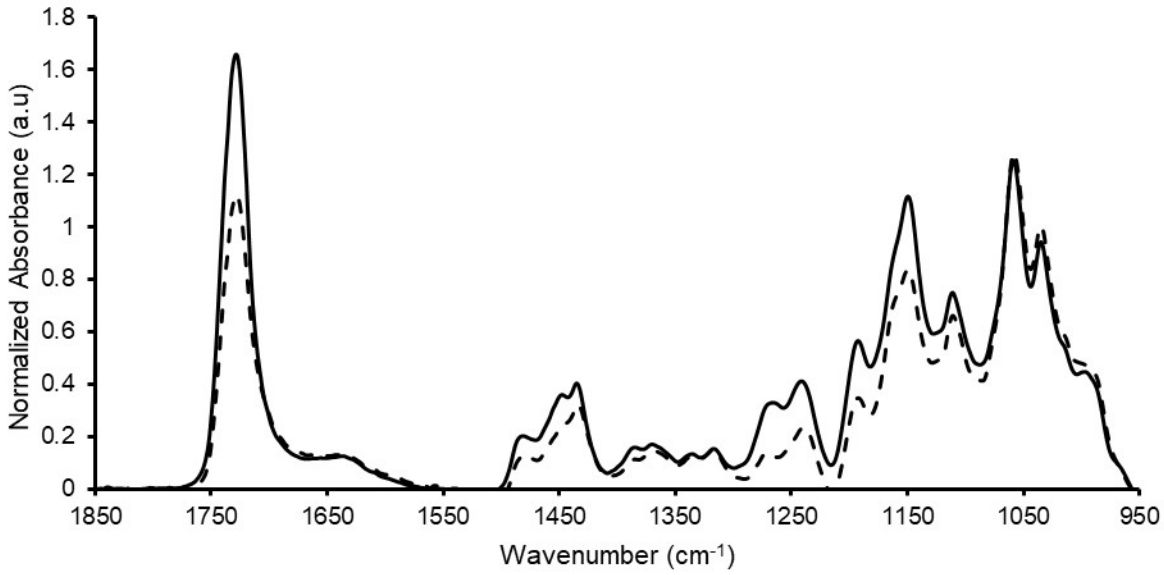

Figure S4. Representative ATR-FTIR spectra of PMMA-FNFs synthesized at 0.5 wt% using FNF-90 after only water washing (solid line) and after washing with DCM (dashed line) to remove the non-covalently bound PMMA.

Table S1. Comparison of band ratios for small-scale and large-scale syntheses of PMMA modified FNFs and CNFs at 0.7 wt% solids.

Label	Total Band Ratio[a] (small scale)	Covalent Band Ratio[b] (small scale)[b]	Total Band Ratio[a] (large scale)	Covalent Band Ratio[b] (large scale)	PMMA wt%[c] (large scale)
FNF-600	1.2 ± 0.1	0.91 ± 0.03	1.6	0.9	42 ± 6%
FNF-900	1.8 ± 0.2	1.14 ± 0.06	1.5	1.0	41 ± 6%
FNF-1350	1.9 ± 0.3	1.5 ± 0.3	2.0	1.6	48 ± 7%
CNF	1.3 ± 0.1	0.9 ± 0.2	1.6	1.0	42 ± 6%

[a]Band ratio of band at 1730 cm^{-1}, corresponding to C=O bond of PMMA, and band at 1055 cm^{-1}, corresponding to the C3 C-O bond of cellulose, after only water washes. [b]Band ratio of band at 1730 cm^{-1}, corresponding to C=O bond of PMMA, and band at 1055 cm^{-1}, corresponding to the C3 C-O bond of cellulose, after washing with DCM. [c]The wt% of PMMA in the polymer modified reinforcement as added to the PLA composite, which was calculated using a calibration curve and method generated in a previous publication.[1]

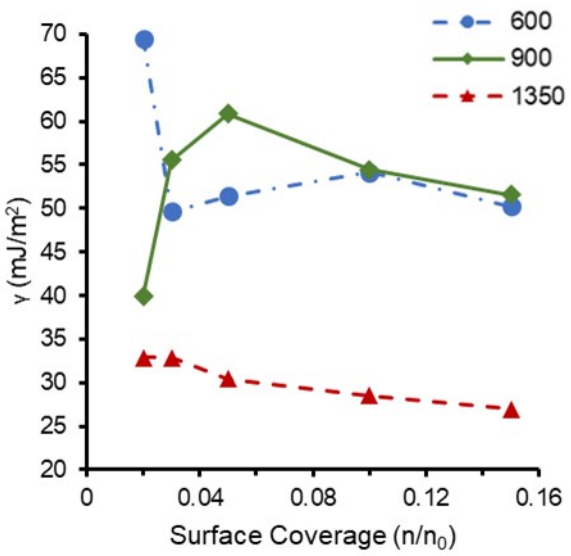

Figure S5. Total surface energy (γ) as a function of fractional molar surface coverage of the probe molecule (n/n_0) for FNF refining energies of 600 (blue circles, dot-dashed line), 900 (green diamonds, solid line), and 1350 (red triangles, dashed line) kWh/MT.

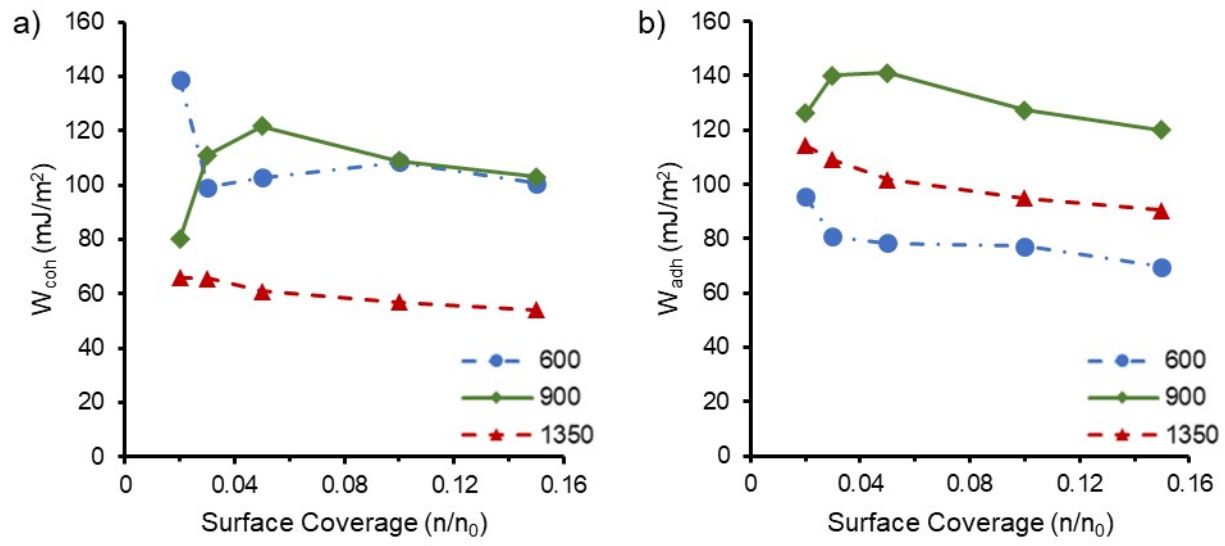

Figure S6. a) The work of cohesion (W_{coh}) and b) work of adhesion (W_{adh}) between the PMMA-FNFs and PLA as a function of fractional molar surface coverage of the probe molecule (n/n_0) for FNF refining energies of 600 (blue circles, dot-dashed line), 900 (green diamonds, solid line), and 1350 (red triangles, dashed line) kWh/MT.

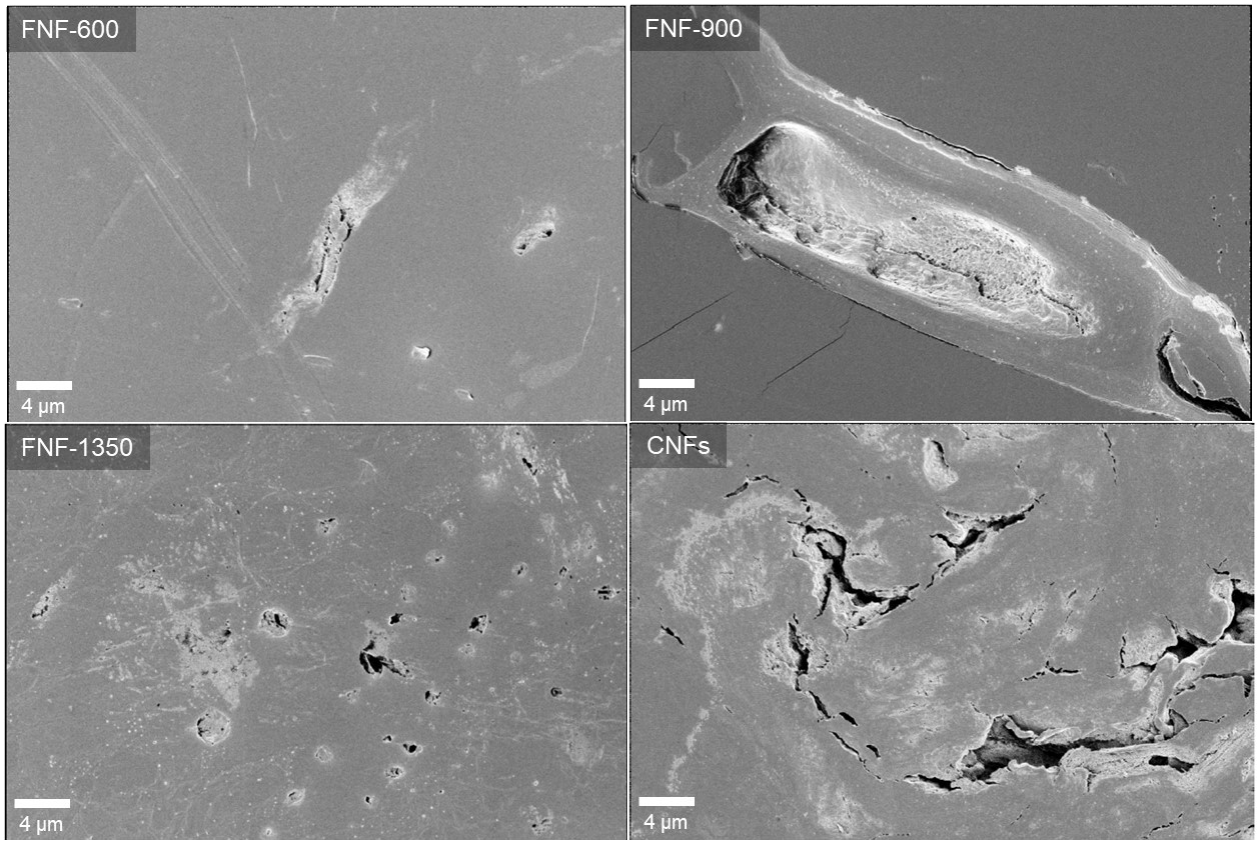

Figure S7. SEM images of composites with 5 wt% PMMA-CNF or PMMA-FNF reinforcements. Samples were polished prior to imaging.

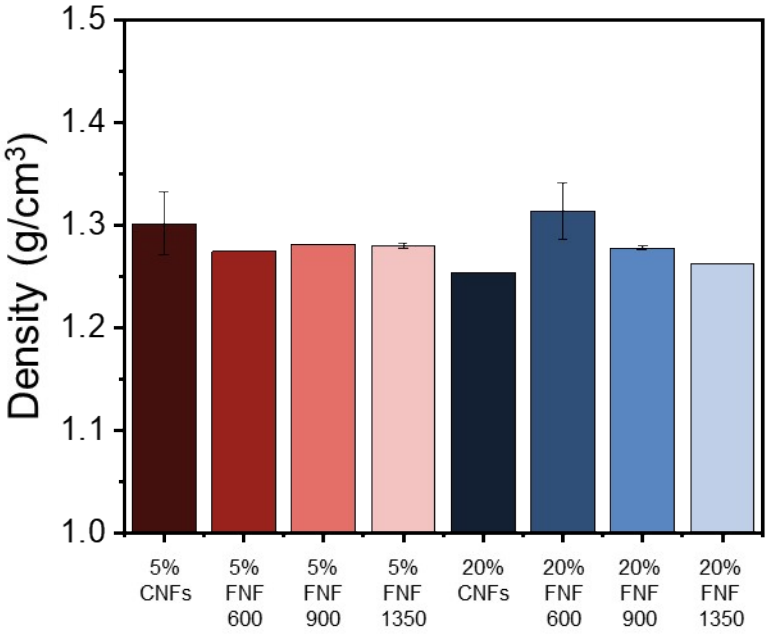

Figure S8. Measured densities of PMMA-CNF and PMMA-FNF composites.

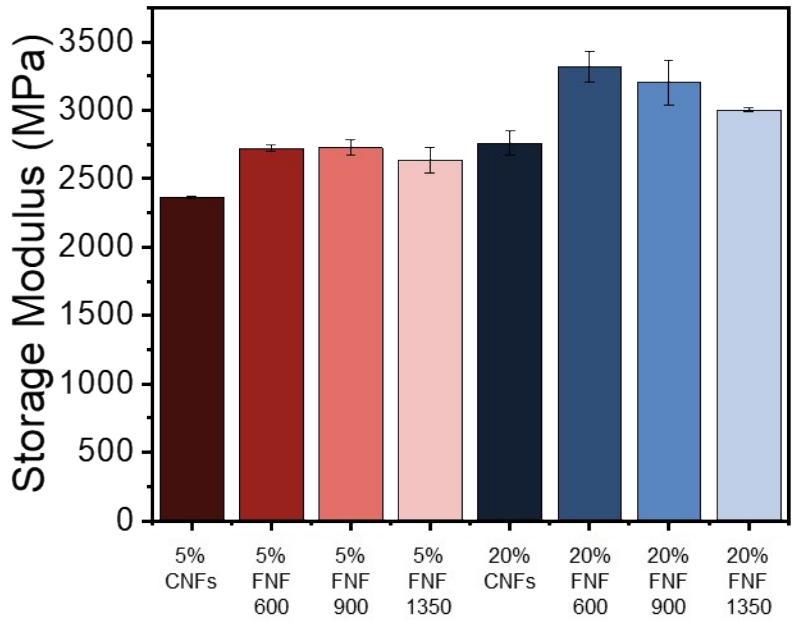

Figure S9. Storage modulus at 35 °C measured during DMA experiments. Error bars are standard deviation (n=2).

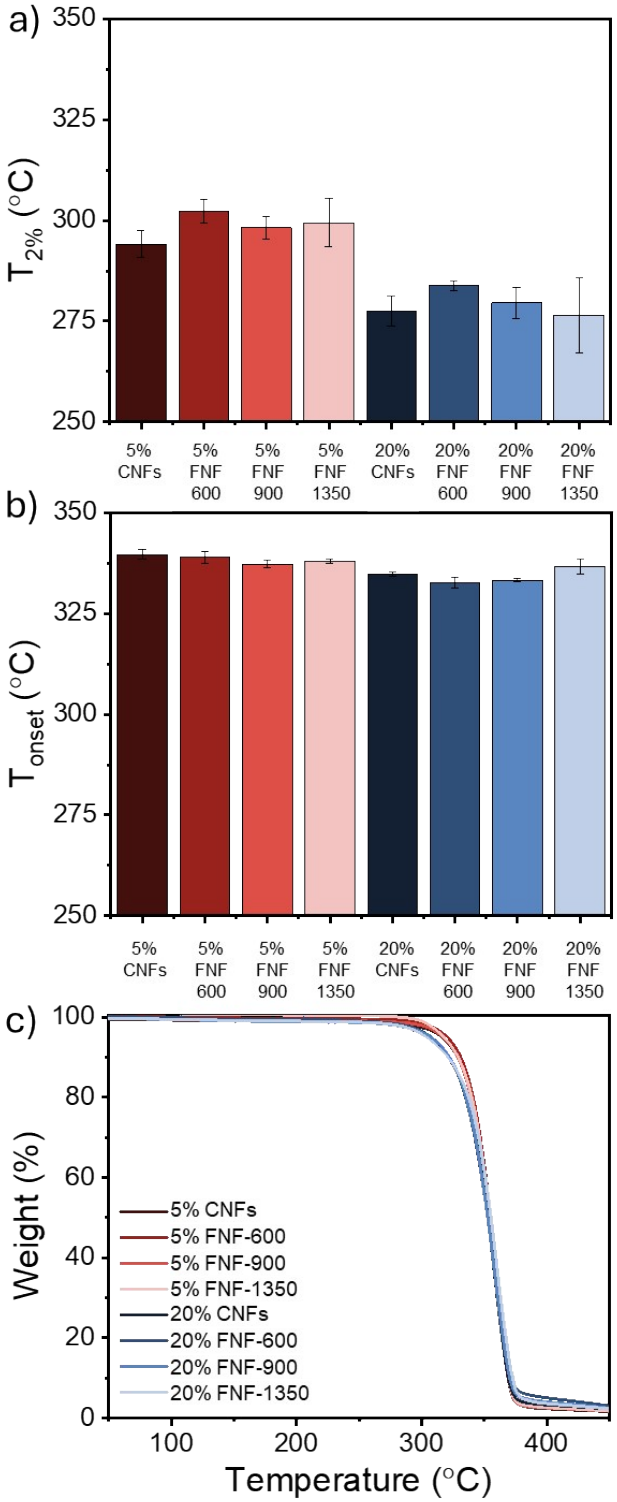

Figure S10. a) Temperature where 2 wt.% ($T_{2\%}$), b) the onset of thermal degradation (T_{onset}), and c) the TGA thermograms for composites made with PMMA-FNFs made from FNFs made at different refining energies and PMMA-CNFs.

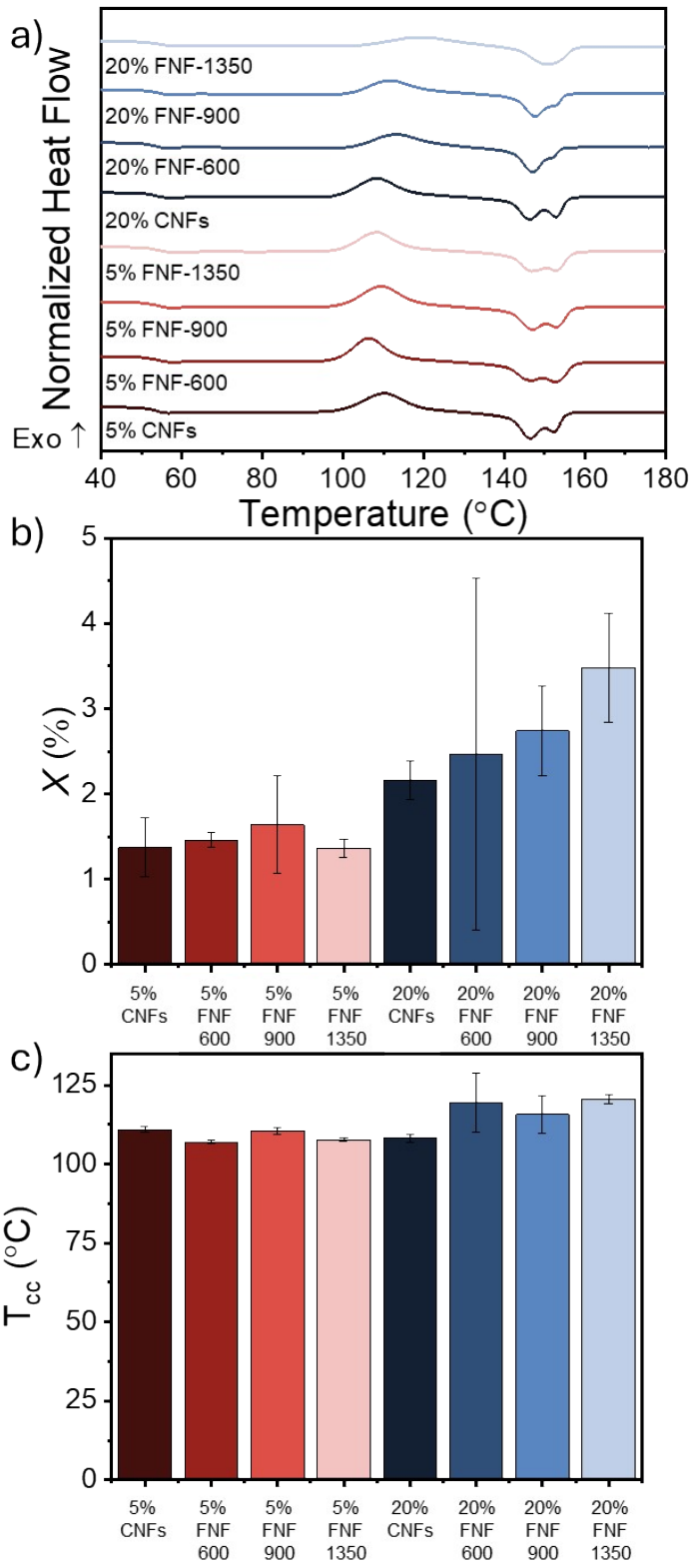

Figure S11. a) DSC thermograms of second heating curve, b) percent PLA crystallinity (X), and c) cold crystallization temperature (T_{cc}) of for composites made with PMMA-FNFs made from FNFs made at different refining energies and PMMA-CNFs.

References

1 P. V. Kelly, P. Cheng, D. J. Gardner and W. M. Gramlich, *Macromol. Rapid Commun.*, 2021, **42**, 2000531.